The Astrophysical Journal, 684:1210–1220, 2008 September 10

FORMATION OF INTERSTELLAR OCS: RADIATION CHEMISTRY AND IR SPECTRA OF PRECURSOR ICES

Robert F. Ferrante,[1] Marla H. Moore,[2] Morgan M. Spiliotis,[1] and Reggie L. Hudson[3]

Received 2008 March 10; accepted 2008 May 17

ABSTRACT

Extensive experimental studies have been performed on the solid-state formation of the OCS molecule in proton-irradiated water-free and water-dominated ices containing CO or CO_2 as the carbon source and H_2S or SO_2 as the sulfur source. In each case OCS is readily formed. Production efficiency follows the trends CO > CO_2 and H_2S > SO_2 as C,O- and S-sources, respectively. In water-dominated ices, OCS production appears to be enhanced for CO : H_2S reactants. The mechanism of formation of OCS appears to be the reaction of CO with free S atoms produced by fragmentation of the sulfur parent species. While OCS is readily formed by irradiation, it is also the most easily destroyed on continued exposure. In H_2O-dominated ices the half-life of H_2S, SO_2, and OCS is ~2 eV molecule^{-1}, corresponding to ~7 million years in a cold dense interstellar cloud environment processed by cosmic-ray protons. The spectral profile of the ν_3 band of OCS is highly dependent on temperature and ice composition, and changes with radiation processing. These effects can be used in theoretical modeling of interstellar infrared (IR) spectra; a laboratory spectrum of irradiated H_2O : CO : H_2S, warmed to 50 K, provides a good fit to the 2040 cm^{-1} feature in the W33A spectrum. The identification of OCS in CO_2-dominated ices provides a further challenge, due to the overlap of the OCS band with that of CO_3 formed from irradiation of the host ice. The two features can be unraveled by a curve-fitting procedure. It is the width of the 2040 cm^{-1} band that will help observers determine if features identified in CO_2-rich ices are due to OCS or to CO_3.

Subject headings: astrochemistry — ISM: molecules — methods: laboratory — techniques: spectroscopic

1. INTRODUCTION

Carbonyl sulfide, OCS, is a molecule that has been identified in a variety of natural environments, both terrestrial and extraterrestrial. It is a component of terrestrial volcanic plumes as well as deep-sea vents and has been found in Antarctic ice cores (Aydin et al. 2002). Recently OCS has been shown to catalyze the coupling of amino acids to produce peptides (Leman et al. 2004), giving the molecule an astrobiological significance.

In extraterrestrial environments OCS has been found in the Venusian atmosphere (e.g., Kamp & Taylor 1990), has been observed in Jupiter's atmosphere (comet D/Shoemaker Levy 9 post collision; Weaver 1997), and has been detected in cometary comae (Mumma et al. 2003; Woodney et al. 1997). Beyond the solar system, OCS has been identified in the infrared spectra of ices in several dense molecular clouds. It is detected in radio observations of gas-phase molecules in the interstellar medium (Charnley et al. 2001 and references therein) and in several extragalactic starburst galaxies (Martin 2005). The relative abundances of OCS in the gas of a cold molecular cloud (L134N), in protostellar ices, in the Orion hot core, and in cometary coma (Hale-Bopp) are shown in Table 1. These observed abundances are snapshots of dynamic chemistry in which solid- and gas-phase OCS and other sulfur-containing molecules are affected by time, temperature, and the surrounding radiation environment.

In laboratory infrared spectra, OCS ice at 10 K shows an intense absorption band due to the ν_3 C = O stretch, and it was this feature that was used to identify OCS as the absorber for the 2041 cm^{-1} (4.9 μm) line in W33A (Palumbo et al. 1995) and in several YSOs (Palumbo et al. 1997; Charnley et al. 2001). Earlier studies by Hudgins et al. (1993) examined the mid-infrared spectrum of pure OCS as well as binary mixtures of OCS in H_2O, CO, and CO_2. The intrinsic strength of the 4.9 μm band of OCS ice was found to rival that of the 4.2 μm band of CO_2 and the 3 μm H_2O feature. Laboratory infrared (IR) studies of H_2O and CH_3OH ices containing OCS were performed by Palumbo et al. (1997) to examine shifts in the OCS band's position and width. Their results suggest that in W33A, OCS is embedded in CH_3OH-rich ices.

Aside from OCS in ice mantles, hydrogen sulfide (H_2S) and sulfur dioxide (SO_2) also have been assigned to observed interstellar IR features. A weak absorption at 3.9 μm in W33A is attributed to H_2S ice (Smith 1991; Geballe 1991) and the 7.58 μm feature in the spectrum of W33A, NGC 7548 IRS 1 is attributed to SO_2 mixed with CH_3OH (Boogert et al. 1997).

In all, there are 15 sulfur species known from interstellar observations (Lovas & Dragoset 2004), while the principal sulfur gas-phase molecules detected in both interstellar environments and cometary comae are SO, SO_2 (sulfur dioxide), H_2S, CS, and H_2CS (thioformaldehyde). Models to predict the SO, SO_2, and CS abundances in several hot-core environments (Charnley 1997; Hatchell et al. 1998) have been based on H_2S-driven gas-phase chemistry. However, OCS abundances have not been reproduced by these gas-phase reaction networks, and therefore, a mantle origin is implied (Charnley 1997, 2004: Hatchell et al. 1998). Furthermore, in dark clouds and star-forming regions, the gas-phase OCS abundance is less than that observed in the solid state, consistent with the molecule's formation by active ice-grain chemistry (see Palumbo et al. 1997 and references therein).

It is thought that icy grain mantles, formed by the accretion of gas-phase species, can undergo both ultraviolet (UV) and cosmic-ray processing and form other more complex molecules (Grim & Greenberg 1987; Palumbo & Strazzulla 1993; Moore & Hudson 2006). However, sorting out likely condensed-phase reactants and

[1] Chemistry Department, US Naval Academy, 572 Holloway Road, Annapolis MD 21402.
[2] NASA Goddard Space Flight Center, Code 691, Greenbelt, MD 20771.
[3] Department of Chemistry, Eckerd College, 4200 54th Avenue South, St. Petersburg, FL 33711.

TABLE 1

ABUNDANCES, RELATIVE TO H_2O AND CO, OF TRIATOMIC SULFUR-CONTAINING MOLECULES IN INTERSTELLAR AND COMETARY ENVIRONMENTS

Object	Phase	Molecule		
		OCS	H_2S	SO_2
W33A	ice*	0.04[a]	<0.2[a,b]	0.31 ± 0.16[c]
AFGL 989	ice*	0.1[d]	...	...
Mon R2 IRS 2	ice*	0.055[d]	<0.5[f]	...
NGC 7538 IRS 1	ice*	...	...	0.8 ± 0.2[c]
NGC 7538 IRS 9	ice*	0.05[e]	...	<0.5[c]
L1234N[e]	gas**	0.02	0.01	0.005
Orion hot core[e]	gas**	0.5	1	0.6
Comet Hale-Bopp[e]	gas*	0.5	1.5	0.1

NOTE.—Abundances denoted by one asterisk (*) are relative to H_2O, and those with two asterisks (**) are relative to CO.

[a] Values from Palumbo et al. (1995).
[b] Values from Geballe et al. (1985).
[c] Values from Boogert et al. (1997).
[d] Values from Palumbo et al. (1997).
[e] Values from Charnley et al. (2001).
[f] Values from Smith (1991).

paths that could contribute to OCS formation requires input from laboratory experiments. Numerous investigations have examined the radiation-induced chemistry of ices containing the more abundant carbon-containing species, such as CO, CO_2, and CH_3OH both with and without water (e.g., Moore et al. 1996; Hudson & Moore 1999), but far less has been done with SO_2- and H_2S-containing ices. Only a few experiments with sulfur-containing molecules are available at interstellar cloud temperatures (e.g., Salama et al. 1990; Schriver-Mazzuoli et al. 2003; Grim & Greenberg 1987; Moore 1984). Moore et al. (2007) showed that MeV ion irradiation of SO_2 and H_2S in H_2O-rich ice at 86–130 K results in the sulfur-containing molecules undergoing an increase in the sulfur's oxidation state and forming sulfuric acid hydrates on warming. However, much less is known about the chemistry of ices in which OCS, SO_2, or H_2S are present in the same mixture as carbon-containing molecules (e.g., CO or CO_2).

In light of the scarcity of data on likely formation steps for OCS in the solid phase, we report new results from experiments on ices containing either CO or CO_2 along with sulfur species H_2S or SO_2, both with and without H_2O. We also present new results on the radiation destruction of condensed-phase H_2S, SO_2, and OCS both pure and in the presence of water, and results on the thermal stability of OCS in various ice mixtures.

2. EXPERIMENTAL METHODS

In our work we studied ices using the mid-IR spectral region, since it contains strong diagnostic IR absorptions of molecules, making it the prime region for product identification. The concentration ratios for ice mixtures examined were typically CO/(SO_2 or H_2S) = 5. This composition was chosen simply to provide measurable product signals in a reasonable irradiation time, rather than to represent any specific astrophysical environment. Proton irradiations of mixtures were done at 10 K, consistent with the low-temperature environment of molecular cloud regions.

Details of our experimental setup, ice preparation, IR spectral measurements, cryostat, and proton beam source have been published (e.g., Hudson & Moore 2004; Moore & Hudson 2003). Briefly, gas mixtures were prepared in a vacuum manifold and then condensed onto a precooled, aluminum mirror inside a stainless-steel high-vacuum chamber ($\sim 10^{-7}$ torr). Appropriate control experiments were done by warming unirradiated ice mixtures to check for possible thermally induced reactions. In no case was a residual material formed in an unirradiated ice. Prolonged exposure of the sample ices to H_2O or other contaminants outgassing from the chamber walls may have induced insignificant changes to the sample composition, but had no effect on the experimental results.

Gas mixtures were condensed and irradiated at 10 K and then warmed while taking spectra to document the stability of volatiles within the ice. Samples could be maintained at any temperature from ~10 to 300 K depending on the ice composition. IR spectra with a range of 4000–400 cm^{-1} (2.5–25 μm) and a resolution of 4 or 1 cm^{-1} were taken by diverting the beam of the Fourier-transform infrared (FTIR) spectrometer (Bruker Vector 22 or Nicolet Nexus) toward the ice film. The beam passed through the ice before and after reflecting at the ice-mirror interface, and then went on to an IR detector. Most ice films examined were 3–5 μm thick, as determined by a laser interference fringe system.

Ices were processed by turning the sample mirror to face a beam of 0.8 MeV protons generated by a Van de Graaff accelerator. Radiation doses were determined by measuring the proton fluence (p^+ cm^{-2}) in the metal substrate beneath the ice sample and then converting to a common scale of electron volt per 16 amu molecule, referred to as simply eV $molecule^{-1}$ in the remainder of this paper. The eV per 16 amu scale was primarily chosen so that our results could directly be compared to previously published data. Stopping powers were calculated with Ziegler's SRIM program (Ziegler et al. 1985)[4] to be 233.6, 221.9, and 216.1 MeV cm^2 g^{-1} for the sulfur species H_2S, OCS, and SO_2, respectively, and 289.0, 245.7, and 240.4 MeV cm^2 g^{-1} for the host ice species H_2O, CO, and CO_2, respectively. The stopping power for mixtures was computed as a composition-weighted average of the stopping powers of the pure components. In all cases, a density of 1.00 g cm^{-3} was assumed for stopping power computations. The intrinsic band strengths (A) of H_2S and SO_2 were required in order to calculate column densities N of the sulfur molecules according to the relation

$$N = \frac{\int \tau(\tilde{\nu}) d\tilde{\nu}}{A} \quad (1)$$

Column densities were then used to determine relative production yields of OCS in different radiation experiments. The A-values employed were those determined by Hudgins et al. (1993) for the pure ices at 10 K: $A(\mathrm{OCS}, 2025\ \mathrm{cm}^{-1}) = 1.5 \times 10^{-16}$ cm $molecule^{-1}$, $A(\mathrm{H_2S}, 2545\ \mathrm{cm}^{-1}) = 2.9 \times 10^{-17}$ cm $molecule^{-1}$, and $A(\mathrm{SO_2}, 1336\ \mathrm{cm}^{-1}) = 3.8 \times 10^{-17}$ cm $molecule^{-1}$. Band areas were calculated from IR spectra by integrations over 2593–2437 cm^{-1} for H_2S and 1350–1300 cm^{-1} for SO_2. The OCS product band areas were determined by integration in the range 2067–2015 cm^{-1}. In some cases, especially for CO_2-containing ices, the OCS line was blended with that of CO_3, another radiation-induced product. In those cases the OCS band area was obtained by a deconvolution procedure as described below.

Reagents used and their sources and purities were as follows: H_2O (triply distilled, with a resistivity greater than 10^7 ohm cm), SO_2 (Matheson, 99.98%), H_2S (Matheson, 99.5%), OCS (K & K Laboratories, purity unspecified), CO_2 (Matheson, 99.995%), and CO (Matheson, 99.99%). For OCS, a trace amount of CS_2 was the only IR-active impurity identified. Separate experiments indicated that CS_2 is much more stable to irradiation than is

[4] See Web site at http://www.srim.org.

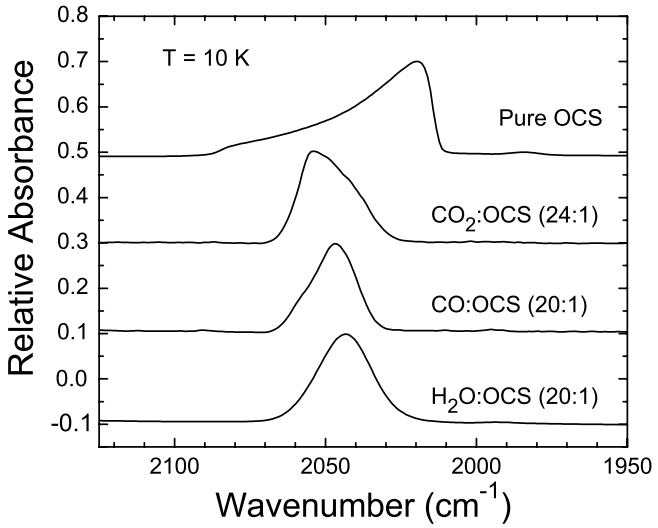

FIG. 1.—IR absorption spectra of solid OCS and OCS mixed with CO, CO_2, and H_2O, all at $T = 10$ K. The OCS peak intensity has been normalized to ~0.2 absorbance units and spectra are stacked for comparison. Table 2 lists peak positions and FWHM values.

TABLE 2

POSITIONS AND FWHM VALUES OF THE ν_3 BAND OF OCS IN ICES FORMED AT ~10 K AND THEN WARMED

Ice Composition	T (K)	OCS Peak Position (cm^{-1})	OCS FWHM (cm^{-1})
Pure OCS	10	2020	29
	25	2019	28
	50	2019	24
	70	2004	25
CO:OCS	11	2047	19
20:1	20	2047	19
CO_2:OCS	11	2054	23
24:1	25	2054	20
	50	2055	15
	70	2055	15
H_2O:OCS	11	2046	18
20:1	25	2046	16
	50	2046	16
	75	2047	13
	100	2047	12
	120	2047	10

OCS, so the presence of trace amounts will have no effect on our results.

3. RESULTS

Although our main interest is in understanding the spectra and chemistry of irradiated ices leading to the formation of OCS, we first present background IR data for unirradiated pure OCS and for OCS in CO- and CO_2-rich ices. Then we present our results involving binary mixtures $CO:H_2S$ and $CO:SO_2$. We also comment on similar experiments in which the carbon source is CO_2 instead of CO. Finally, we examine the more complex three-component mixtures $H_2O:CO:(H_2S$ or $SO_2)$.

3.1. *Unirradiated Ices*

The IR spectra of the ν_3 band of pure OCS and mixtures of $CO:OCS$ (20:1), $CO_2:OCS$ (24:1), and $H_2O:OCS$ (20:1) in the 2150–1950 cm^{-1} region are shown in Figure 1. The peak position for OCS in these ices at 10 K is listed in Table 2 along with band positions and full width at half-maximum values (FWHM; measured in absorbance) during warming. The OCS ice sample was amorphous at 10 K and began to crystallize near 30 K. Slow-warming experiments showed that pure OCS vaporized quickly in our vacuum system near 80 K (CO near 30 K and CO_2 near 90 K), although OCS could be trapped in H_2O ice up to 120 K. Our spectra at 10 K for pure OCS ice and OCS in CO, CO_2, and H_2O resemble those published by Hudgins et al. (1993) and by Palumbo et al. (1995). Palumbo et al. (1995) did a detailed study of OCS at different H_2O/OCS ratios and measured band positions and FWHM values; they also looked at the dependence of the OCS position and FWHM in the presence of CH_3OH.

3.2. *Irradiated Sulfur Molecules in* CO *Ices*

Figure 2 shows IR spectra of $CO:H_2S$ (5:1) deposited at 10 K before and after irradiation (dose = 1 eV $molecule^{-1}$). The 2143 cm^{-1} fundamental of CO and 2555 cm^{-1} (ν_1) band of H_2S are indicated. After irradiation OCS (2048 cm^{-1}) and CS_2 (1524 cm^{-1}) are the S,C-containing radiation products identified. Other features such as C_3O_2 (2242 cm^{-1}, carbon suboxide), CO_2 (2343 cm^{-1}), and C_2O (1990 cm^{-1}) were due to the irradiation of the CO ice alone. The HCO radical's presence is shown by a feature at 1859 cm^{-1} (Hudson & Moore 1999). Table 3 gives the OCS peak position and FWHM in the irradiated ice at 10 K and during warming. Table 4 lists all of the identified radiation products and their band positions.

Figure 3 shows IR spectra of $CO:SO_2$ (5:1) deposited at 10 K before and after irradiation (dose = 1 eV $molecule^{-1}$). The ν_3 and ν_1 bands of SO_2 at 1337 and 1152 cm^{-1}, respectively, are indicated. After irradiation OCS (2049 cm^{-1}) is the only S,C-containing radiation product identified (see Table 3 for band position and FWHM during warming). A new sulfur species is SO_3 (1401 and 1393 cm^{-1}). The same carbon oxide features seen in Figure 1 also are found. See Table 4 for a list of the identified radiation products and their band positions.

A comparison of the OCS bands in irradiated CO-rich ices containing H_2S or SO_2, with and without H_2O, is shown in Figure 4. The initial ratio of CO : sulfur species was typically 5:1 and the ratio of $H_2O:CO:$ sulfur ranged from 2:2:0.2 to 2:2:0.02. All ices were irradiated at 10 K to a total dose of 1×10^{14} p^+ cm^{-2},

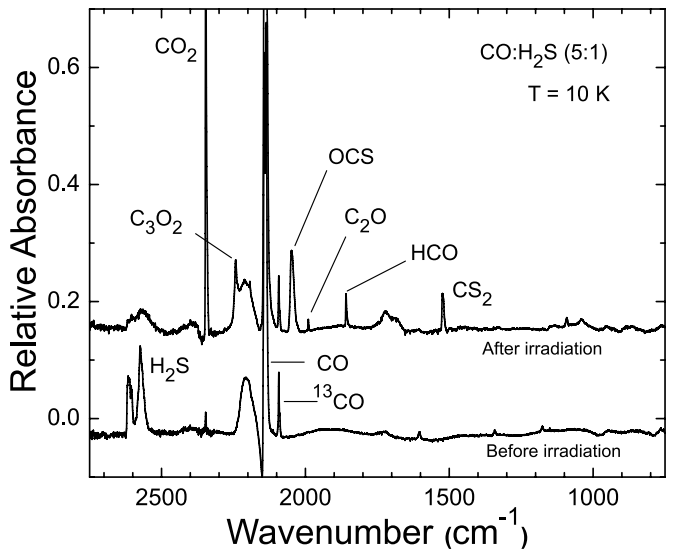

FIG. 2.—Mid-IR spectrum of $CO:H_2S$ before and after irradiation to a dose of 1 eV $molecule^{-1}$.

TABLE 3
Positions and FWHM Values of the ν_3 Band of OCS Formed in Ices Irradiated at ~10 K and Then Warmed

Ice Composition	Radiation Dose (p^+ cm^{-2})	T (K)	OCS Peak Position (cm^{-1})	OCS FWHM (cm^{-1})
$CO:H_2S$	3.5×10^{14}	10	2048	18
5:1		50	2037	19
		100	2036	19
		150	2034	16
$CO:SO_2$	3.5×10^{14}	10	2049	17
5:1		25	2048	15
		50	2043	18
		75	2043	18
		100	2041	19
		125	2041	14
$H_2O:CO:SO_2$	1.5×10^{15}	10	2044	17
10:5:0.2		50	2043	16
		100	2044	14
		150	2046	10
$H_2O:CO:H_2S$	3.5×10^{14}	10	2045	16
8:4:0.8		50	2037	18
		100	2037	19
		150	2035	17

which corresponds to ~1 eV molecule^{-1}. In Figure 4, the individual band intensities have been adjusted to be approximately equal in each trace, in order to focus on band position and width. The actual intensities for the irradiated samples varied with the sulfur and carbon parent molecules, even for the same temperature and radiation dose. The effect of the source on the production rate of OCS is discussed in § 3.4. Reference spectra of CO- and H_2O-rich ices containing OCS are included for comparison.

3.3. *Irradiated Sulfur Molecules in* CO_2 *Ices*

Corresponding to the work just described, where CO was used as the carbon source, similar experiments were conducted by irradiating ices formed from binary mixtures of $CO_2:H_2S$ or $CO_2:SO_2$ with an initial ratio of CO_2 : sulfur species of 5 : 1. In each case, OCS was identified after irradiation. A comparison of products identified in CO- and CO_2-rich ices is given in Table 4

TABLE 4
Products Identified in Irradiated C,O,S-containing Ices

	SO_2		H_2S	
C,O source	Product	Position (cm^{-1})	Product	Position (cm^{-1})
CO.....	CO_2	2343	CO_2	2343
	C_3O_2	2242	C_3O_2	2242
	OCS	2049	OCS	2048
	C_2O	1990	C_2O	1990
			HCO	1859
			H_2CO	1712, 1496
			CS_2	1524
	SO_3	1401, 1393		
	SO	1130		
	O_3	1040	O_3	1040
CO_2.....	CO	2142	CO	2142
	OCS	2048	OCS	2048
	CO_3	2043	CO_3	2043
	SO_3	1402, 1392		
			SO_2	1337, 1152
	O_3	1039	O_3	1044

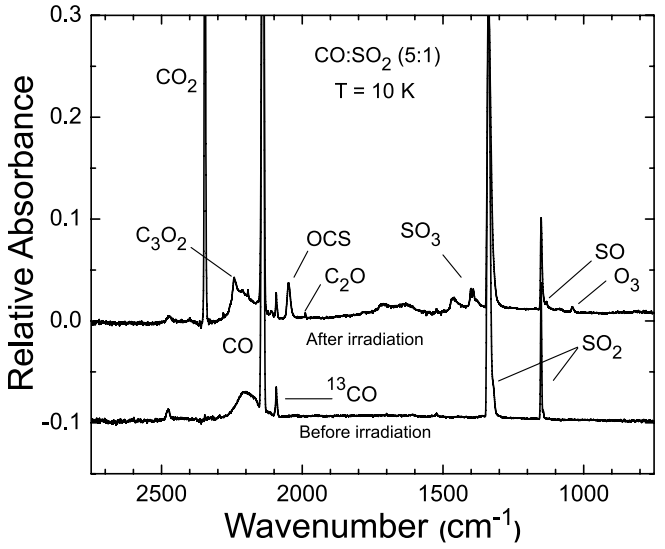

Fig. 3.—Mid-IR spectrum of $CO:SO_2$ before and after irradiation to a dose of 1 eV molecule^{-1}.

along with peak positions. In general, the rate of OCS formation from CO-rich ices was greater than that observed in CO_2-rich ices, as described in § 4.1.

Only CO_2-rich ices formed ozone, O_3, and carbon trioxide, CO_3 (Jacox & Milligan 1971; Hudson et al. 2007; Bennett et al. 2004) in significant amounts. The ν_1 (C = O stretch) of CO_3, at 2043 cm^{-1} frequently was blended with that of the OCS product. The radiation behavior of these two species differed, with OCS typically growing and then decaying with increasing dose, and CO_3 continuing to grow as the irradiation proceeded. The characteristics of the spectroscopic features associated with these molecules also differed. The CO_3 molecule has a symmetrically shaped band whose position and FWHM in pure CO_2, and in $CO_2:OCS$, NH_3, and $CO_2:H_2O$ ranges from 2044 to 2045 cm^{-1} in position and from 4.5 to 8.7 cm^{-1} in FWHM. The FWHM of the synthesized OCS band appearing in the 2044 cm^{-1} region in irradiated

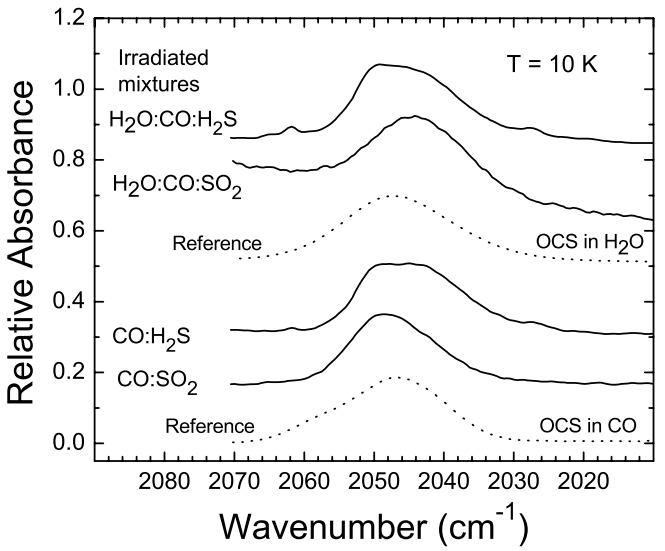

Fig. 4.—Stacked spectra compare the shape and position of the OCS band formed in different irradiated ices. Binary anhydrous ices are compared with tertiary ices containing H_2O. Peak positions and FWHM values of these spectra are in Table 3. Reference spectra of CO- and H_2O-rich ices containing OCS are shown for comparison. See Table 2 for peak positions and FWHM values.

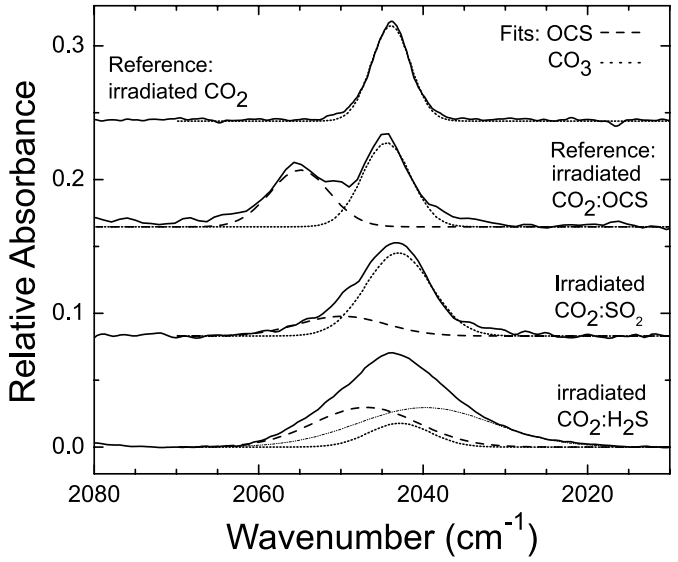

FIG. 5.—The 2043 cm^{-1} absorption feature for these irradiated CO_2-rich ice mixtures can be fitted with two peaks suggesting the presence of both CO_3 and OCS.

CO_2-dominated ices is greater (typically 11.5–19 cm^{-1}) than the width expected for CO_3 only. Isotopic labeling experiments could not distinguish between the two, so the component due to OCS was calculated using curve-fitting techniques to separate the overlapping features. These fits used the consistency in the width, shape, and position of the CO_3 band to distinguish it from the more-variable OCS feature. Figure 5 illustrates several examples of the results of the fitting procedure. Each of the sulfur-containing ices in the figure was irradiated to approximately the same dose of 1 eV $molecule^{-1}$. The top trace shows the spectrum obtained after irradiation of a pure CO_2 ice; the strong feature is the ν_1 band of CO_3 and serves as a reference point for the other spectra. It is characterized by a very symmetric shape and by a line width (FWHM) near 6 cm^{-1}. The second trace from the top shows the results of irradiating an ice prepared from a CO_2 : OCS (100 : 1) mixture. The CO_3 line is in the same position, but with a slightly larger width (7 cm^{-1}), while the OCS feature is broader and centered at 2055 cm^{-1}. The third trace is from an irradiated ice prepared from a 5 : 1 mixture of CO_2 : SO_2. The OCS feature identified in the fit has shifted substantially and broadened, while the CO_3 line maintains its characteristics. The disparity in behavior of the two features is even more apparent in the bottom trace, from an irradiated ice initially CO_2 : H_2S (5 : 1). Here, the overall band is much broader than in any of the other cases. This feature could not be accommodated by a two-peak fit without requiring an uncharacteristically broad CO_3 component. In addition, at high radiation doses both the high- and low-wavenumber wings of the band decrease, at somewhat different rates, further suggesting that a three-peak fit is appropriate. While the OCS and CO_3 components could be readily modeled with typical positions and line widths observed in other ices, and the maximum CO_3 area could be bounded by the yield expected in irradiation of a CO_2 ice at comparable thickness and dose, the third band was unconstrained. Thus, the fit displayed at the bottom of Figure 5 can only be regarded as an approximate one. Similarly, consistent fits were observed in all samples of OCS (and CO_3) generated in our CO_2-rich irradiated ices. These spectra graphically illustrate the sensitivity of the OCS band to its environment, as suggested in Figures 1 and 4 and Tables 2 and 3. In addition, the relative conversion efficiency of sulfur parent to OCS is clear from the last two traces. In both the CO_2-rich and the CO-rich ices, we observed greater OCS production from H_2S than from SO_2.

3.4. *Comparing* OCS *Formation in Irradiated Ices Containing* H_2S *and* SO_2

Figure 6 shows the relative production of OCS as a function of radiation dose and ice composition. For clarity, the figure is divided into two data groups: one for anhydrous ices, where the dominant species is the carbon source (CO or CO_2), and one for H_2O-dominated ices. In every case, the limiting reagent for OCS formation is the sulfur-containing parent, H_2S or SO_2. For each half of the figure, the points were obtained by dividing the column density of the radiation-produced OCS ν_3 band near 2040 cm^{-1} by the approximate column density of the initial sulfur species, and then normalizing each group of results to the maximum of all traces in the group. This procedure provides an approximation for the trends observed between the different sulfur sources, and between H_2O-rich and H_2O-free ices, as further described below. The initial column density of the sulfur parent served as a measure of the initial number of sulfur atoms available for reaction. These abundances were determined from the areas of H_2S (ν_3 = 2545 cm^{-1}) and SO_2 (ν_3 = 1336 cm^{-1}) bands measured before irradiation, and their respective intrinsic intensity values (A). For the H_2O-free ices, the maximum in the production curve occurred with the CO : H_2S ice at a dose of 1 eV $molecule^{-1}$. At this peak our calculated (OCS/original S) column density ratio was 0.08. For the H_2O-dominated group the maximum occurred with the H_2O : CO : H_2S mixture, again at ~1 eV $molecule^{-1}$. For this ice, our calculated (OCS/original S) column density ratio was 0.12. There are clear differences in the OCS production efficiency for H_2S and SO_2, and between CO and CO_2 ices. While the intrinsic intensity values used to evaluate the initial S-atom amounts depend on both temperature and ice composition, typical variations are under 20% from that of the pure ice for the range of mixtures studied here. Comparing the CO : H_2S and CO : SO_2 traces, the differences clearly exceed this uncertainty. Similarly, the CO : SO_2 ice results clearly differ from those of irradiated CO_2 : SO_2. However, because of the less-constrained three-peak fit required to analyze the CO_2 : H_2S ices, the distinction between them and the CO_2 : SO_2 results are less quantitative. No acceptable fit yielded a smaller OCS component for the H_2S source than the corresponding SO_2, source, but the magnitude of the difference cannot be regarded as quantitatively accurate.

3.5. *Irradiation of* OCS

As illustrated by Figure 6, for most of the ices studied the abundance of the OCS product rises to a peak and then drops off with continued irradiation. This is due, at least in part, to OCS destruction, since it too was being irradiated. To illustrate OCS destruction, Figure 7 shows the changes in the spectrum of a pure OCS ice irradiated at 10 K. The bottom trace shows the pure OCS sample before irradiation. Assignments of the OCS combination bands are based on matrix spectra from Bahou & Lee (2001). The OCS band positions at 2021 (ν_3), 1885 ($\nu_1 + 2\nu_2$), 1709 ($2\nu_1$), 1042 ($2\nu_2$), 857 (ν_1), and 516 (ν_2) cm^{-1} are consistent with the values of Hudgins et al. (1993). Except for weak contaminant bands of CS_2 at 1518 and 654 cm^{-1} in the initial sample, all of the other weak features are OCS combination bands. As the ice was exposed to proton irradiation, OCS was destroyed as strong features of the stable molecules CO (2137 cm^{-1}), CS_2 (1517 and 654 cm^{-1}), and SO_2 (1334 and 1144 cm^{-1}) grew in. These features persisted to the highest doses delivered to the sample. In contrast, the intermediate dithiiranone, OCS_2, grew in and

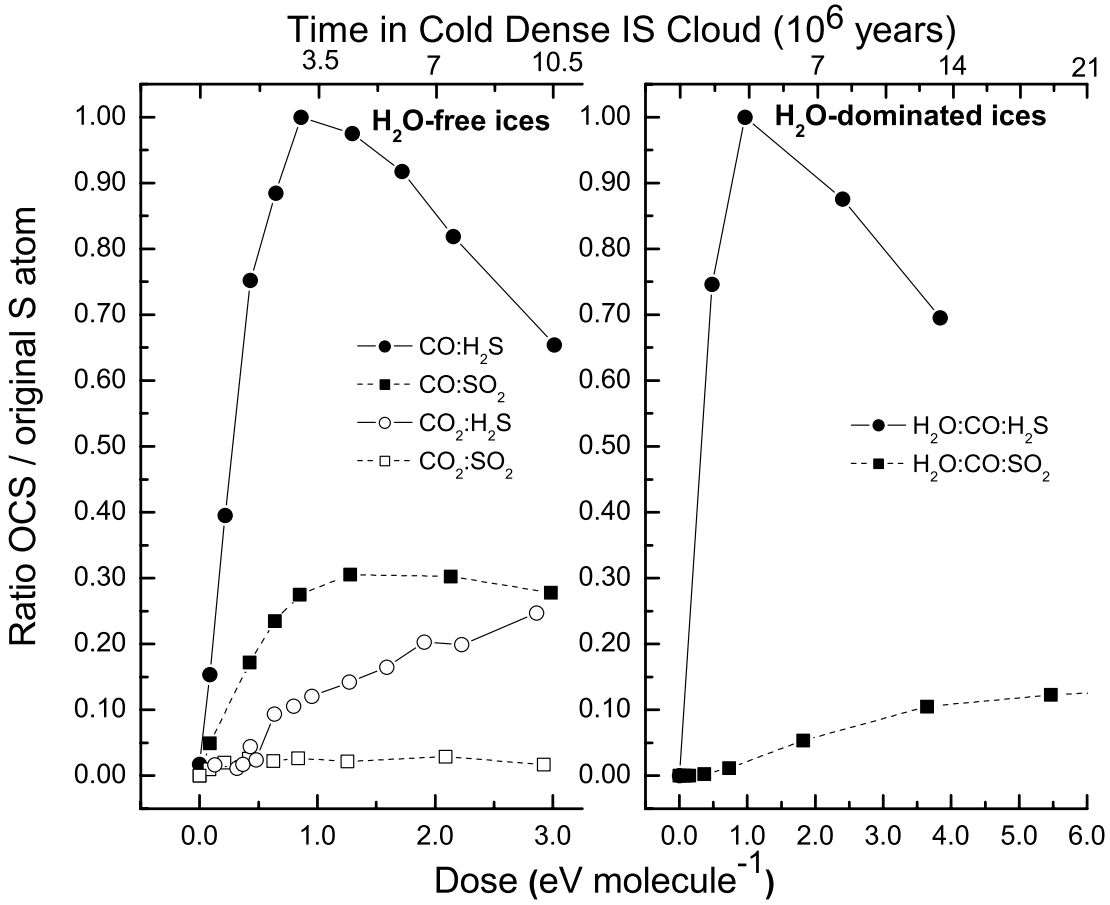

FIG. 6.—Relative formation of OCS in anhydrous binary ices (*left*) compared to OCS formation in the same mixtures but with H_2O added (*right*). Each data set is normalized with respect to the spectrum giving the maximum OCS band area. Irradiations were performed at 10 K.

then decayed with continued irradiation, as indicated by the feature at 1807 cm^{-1}. Its identification is based on matrix spectra of Lo et al. (2004). Observation of this and other intermediates identified earlier was helpful in elucidating possible reaction mechanisms for the solid-state processes observed.

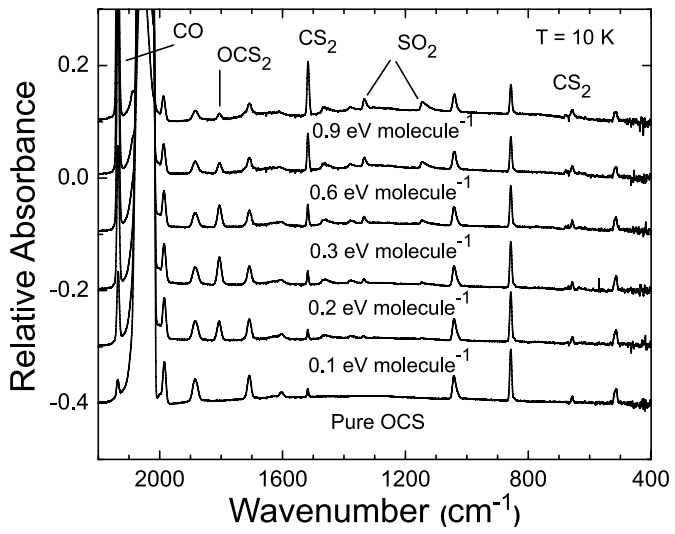

FIG. 7.—Products formed in OCS ice during 0.8 MeV proton irradiation at 10 K. The OCS_2 molecule quickly forms and is then destroyed as the irradiation continues.

3.6. *Radiation Destruction of* H_2S*,* OCS*, and* SO_2 *with and without* H_2O

The radiation destruction of H_2S, SO_2, and OCS ices with and without H_2O was measured at 10 K. Figure 8 plots the relevant sulfur molecule's normalized band area as a function of absorbed dose. We followed the ν_1 H_2S band near 2545 cm^{-1}, the ν_3 SO_2 band near 1336 cm^{-1}, and the ν_3 OCS band near 859 cm^{-1} as a function of dose. Each feature's intensity was normalized to the band area before irradiation. Interestingly, pure SO_2 was relatively immune to destruction by radiation, for the doses we examined, while pure H_2S and pure OCS were highly susceptible. In water-dominated ices (10 : 1 or 5 : 1), SO_2 became much more susceptible to radiation damage, while H_2S and OCS showed only relatively minor increases in destruction rates. Interpretation of these results is provided in § 4.

3.7. *Thermal Behavior*

The irradiations leading to OCS production in various ices, with concomitant destruction of the parent sulfur compounds, were all performed near 10 K. After the terminal radiation exposure, samples were warmed in steps to observe the thermal evolution of the films and the OCS radiation product. Controlled warmings were performed to temperatures of 25, 50, 75, 100, and 120 K in most cases, with additional interim steps for some samples. Samples were typically warmed to the target temperatures in steps, over a period of several minutes, to avoid overshooting . Ices were stabilized at a temperature for several minutes before spectral scans

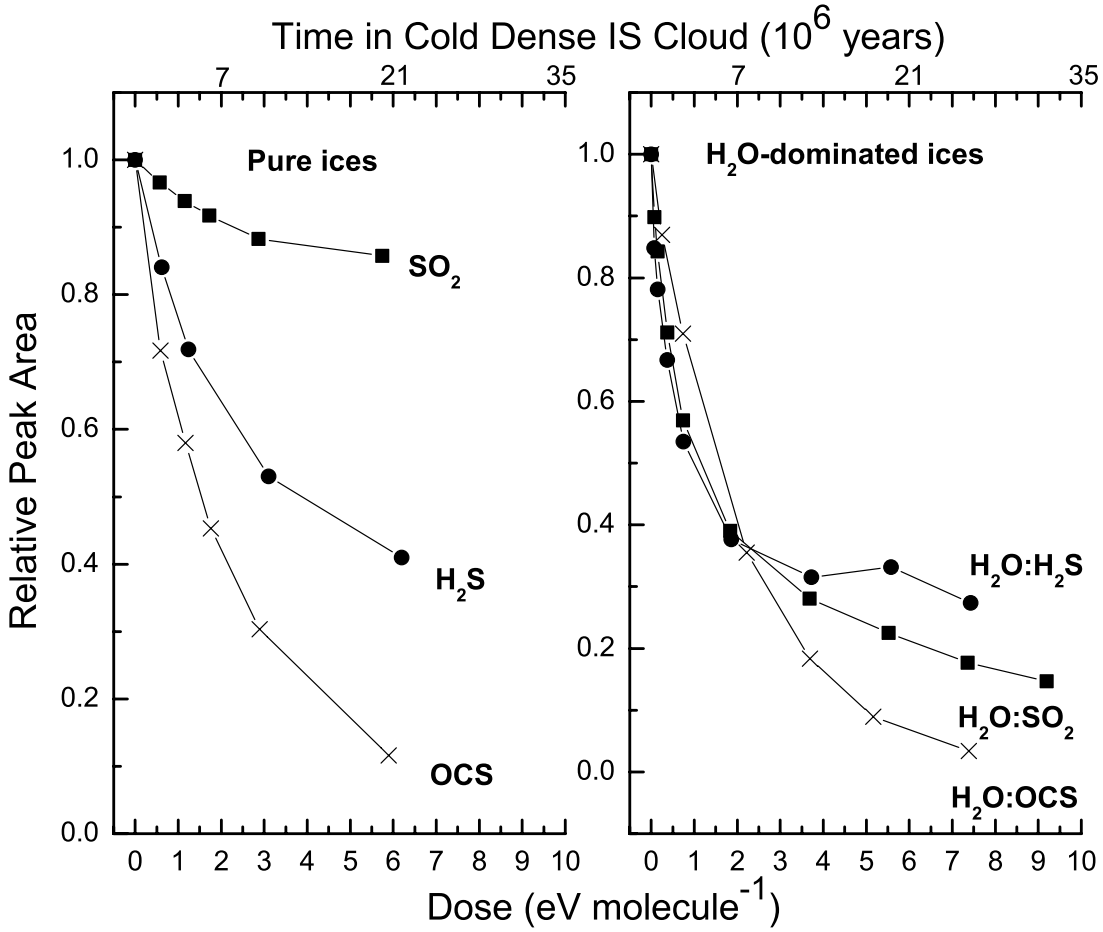

FIG. 8.—Radiation destruction at 10 K of SO_2, H_2S, and OCS, and of those same three molecules in binary mixtures with H_2O.

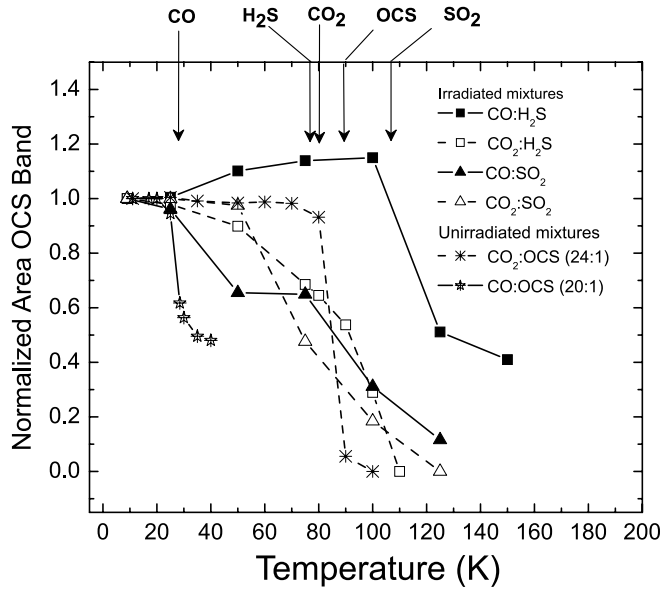

FIG. 9.—Thermal stability of OCS formed in different irradiated ices at 10 K, compared to the change in the OCS band area in unirradiated CO- and CO_2-rich ices. The temperatures of rapid sublimation of pure CO, CO_2, H_2S, SO_2, and OCS ices in our vacuum system are indicated at the top of the graph.

were initiated and generally remained at the temperature for 15 minutes before moving to the next temperature value. The results of those studies are shown in Figure 9, and Table 2 gives the band position and width of OCS as a function of temperature. Each trace in the figure was obtained by measuring the area of the product OCS band and normalizing it to the band area obtained after irradiation at 10 K, but before warming the sample. The lines at the top of the figure mark temperatures corresponding to vapor pressures of 1×10^{-7} torr for the various species indicated. This provides an indication of the temperature at which sublimation of the dominant species in the ice might be expected to become important under the conditions of the dynamic vacuum of our cryostats. In the H_2O-free ices, 40% or more of the OCS was still present well above the sublimation temperature of the CO or CO_2 that dominated those samples. In the case of H_2S in CO, the OCS signal actually *increased* up to about 100 K, indicating that OCS was still being formed from residual species in the ice, in the absence of irradiation. For comparison the thermal evolution of OCS in unirradiated CO_2-rich and CO-rich ices is also shown in Figure 9. In irradiated CO_2-dominated ices, we also observed that the CO_3 band is stable under vacuum to the temperature of sublimation of the CO_2 ice near 90 K (see also Bennett et al. 2004).

4. DISCUSSION

4.1. *Irradiation of Sulfur-Containing Molecules in* CO *and* CO_2 *Ices*

Since the radiation products of the host species CO (Trottier & Brooks 2004) and CO_2 (Hudson et al. 2007; Bennett et al.

2004) are well documented, this discussion concentrates on sulfur-containing products. It is clear from the range of products and behavior of their spectral features that irradiation of our ices at 10 K led to partial or complete fragmentation of the original ice's sulfur-containing compound. The formation of SO_3 from irradiated SO_2 in CO (Fig. 2) suggests scission of one S = O bond in the parent molecule. The idea that SO_2 fragmentation could result in a free O atom is consistent with the identification of a small O_3 signature in CO : SO_2–irradiated ices, a product not found in irradiated pure SO_2 (Moore 1984) or pure CO ices (Trottier & Brooks 2004). The creation of a free S atom is consistent with the identification of OCS in SO_2-containing ices. However, the irradiation of H_2S in CO (Fig. 2) leads to the formation of OCS and CS_2, both of which require complete destruction of the H_2S donor to provide free sulfur.

Irradiation of CO_2-rich ices, containing the same sulfur donors as the CO-rich samples, gave similar products, although they tended to be more highly oxygenated in the CO_2 case. Thus, irradiated H_2S in CO formed CS_2 but no SO_2, while irradiated H_2S in CO_2 formed SO_2 but no CS_2. This is clearly related to the release of free oxygen atoms by fragmentation of the CO_2 matrix molecules. The case for free O atoms is further substantiated by the observation that CO_3 and O_3 were both produced by the irradiation of CO_2 ices.

4.2. *Characteristics of the* OCS *Band*

In unirradiated ices, the band position and FWHM of the OCS band is sensitive to the nature of the matrix ice (CO, CO_2, H_2O), the OCS concentration, and the ice temperature. Typically, our spectra are consistent with those published by Palumbo et al. (1995), as described above. For the (100–10) : 1 ratio ices we studied, the OCS band is in the 2055 cm^{-1} region in solid CO_2, near 2044 cm^{-1} in CO matrices, and around 2040 cm^{-1} in H_2O-ice. Overall in these three cases, we measured OCS widths that ranged from 11.5 to 23 cm^{-1}.

Our results show that OCS can be recognized in irradiated CO-dominated ices in laboratory spectra as a band at 2041–2049 cm^{-1} with a width (FWHM) of 15–18 cm^{-1}. In irradiated H_2O + CO ices containing a source of sulfur, the OCS band falls also within these band positions and widths. The band is thermally stable under vacuum up to the sublimation temperature of the matrix ice.

Laboratory spectra of irradiated CO_2-dominated ices containing a sulfur source reveal a band near 2044 cm^{-1}, but its identification as OCS is complicated by the fact that a primary radiation product of the matrix, the CO_3 molecule, also has its strong ν_1 absorption near this position. While the bands of CO_3 and OCS *initially* present in reference ice spectra were resolvable, OCS produced in situ by exposure to radiation could not be spectroscopically separated from CO_3. This necessitated the use of curve-fitting techniques to deconvolute the spectra, as described in § 3.3. In these cases the fitted OCS component appeared in the range 2047–2050 cm^{-1}, with FWHM in the range 12–16 cm^{-1}. During the fitting process these parameters were permitted to vary outside these ranges by $\sim\pm$3–5 cm^{-1} in most cases.

4.3. *Reactions and Mechanisms for Formation of* OCS *and Other Molecules*

4.3.1. OCS *Formation*

One conceivable solid-phase path to interstellar OCS involves capture of an S atom by CO or in an ice mantle. To our knowledge this pathway has not been demonstrated experimentally for any realistic ice analog until now. The results we report here describe different ways to form OCS, all involving radiation-driven chemistry to generate the sulfur atom.

Our earlier work, and that of others, has shown that in most cases the products of photo- and radiation chemical processing of ices are nearly identical (Hudson & Moore 2000). This equivalence can be understood when it is recalled that the majority of observed radiation-chemical changes are mediated by secondary electrons with energies in the range of UV and vacuum-UV photochemistry. This also allows the present laboratory results to be interpreted in terms of work already in the literature, particularly studies of photolyzed matrix-isolated molecules.

We begin with CO-rich laboratory mixtures, since CO is relatively high in abundance in interstellar ices. Hawkins et al. (1985) have demonstrated that a wide variety of molecules, including CO, are capable of capturing S atoms. Previous experiments also have shown that excited H_2S molecules dissociate into H and HS radicals and that HS undergoes further dissociation to give S atoms (Isoniemi et al. 1999). All of this suggests that our ion-irradiated CO : H_2S mixtures should give rise to OCS, an expectation borne out by Figure 1. The reaction sequence is

$$H_2S \rightarrow 2H + S$$

$$S + CO \rightarrow OCS.$$

Results from the irradiation of CO_2 : H_2S mixtures also are expected to make OCS, but since the needed CO has to come from CO_2 dissociation, the OCS abundance is less, and produced more slowly, than in the case of CO : H_2S ices.

Sulfur dioxide is a second sulfur source we considered for OCS. It is known that SO_2 can dissociate to either O + SO or S + O_2 (Okabe 1978, p. 247), so the OCS we observe in irradiated CO : SO_2 is probably from

$$SO_2 \rightarrow S + O_2$$

$$S + CO \rightarrow OCS.$$

Irradiated ices rich in CO_2 also are expected to follow this sequence once CO has been made.

4.3.2. *Other Products from* SO_2- *and* H_2S-*Containing Ices*

Table 4 summarizes other sulfur molecules seen in our irradiations. For CO : SO_2 and CO_2 : SO_2 mixtures we expected the reactions

$$SO_2 \rightarrow SO + O$$

$$SO_2 + O \rightarrow SO_3$$

to give both SO and SO_3 (Moore 1984), and these products were observed. The irradiated CO_2 : H_2S ice gave SO_2, probably with oxidation of S atoms by an intermediate such as O atoms from CO.

Another interesting sulfur-containing product was CS_2, seen only in irradiated CO : H_2S. Since this mixture was also the one showing the greatest yield of OCS, we suspect that this molecule is linked to CS_2 formation, as explained below.

The remaining product distribution in our CO-rich mixtures is dominated by C_3O_2, C_2O, and CO_2 and has been investigated previously (Trottier & Brooks 2004; Gerakines & Moore 2001). Our irradiated CO_2-rich mixtures contained, aside from sulfur-containing molecules, CO, CO_3, and O_3, which have all been seen in the past (Brucato et al. 1997; Gerakines et al. 1996).

4.3.3. *Radiation Products from* OCS

Reactions competing with $S + CO \rightarrow OCS$ will limit the OCS yield in all cases, as do the destruction reactions of OCS itself. For the latter, Figure 7 shows that irradiated OCS contains OCS_2, CS_2, and SO_2. The easiest way to explain OCS_2 is with the sequence

$$OCS \rightarrow CO + S$$

$$S + OCS \rightarrow OCS_2.$$

Subsequent $OCS_2 \rightarrow O + CS_2$ dissociation will give the CS_2 product. The appearance of SO_2 in irradiated OCS is more difficult to explain. We observed the $OCS \rightarrow SO_2$ conversion only in pure-OCS ices, so

$$2OCS \rightarrow CO_2 + SO_2$$

probably represents the overall process (Hawkins & Downs 1984). Dilution of OCS by any other molecule will reduce the population of OCS pairs that could combine according to the preceding reaction.

4.3.4. *Influence of* H_2O

We now turn from two-component anhydrous ices to the three-component mixture $H_2O : CO : H_2S$. Sulfur atoms from irradiated H_2S can be captured by CO to make OCS, but any H_2O molecules present can oxidize those same sulfur atoms, giving SO_2 (Moore et al. 2007). If the oxidation is sufficiently efficient then it might completely block OCS formation. Figure 6 summarizes the experimental result: OCS formation occurs not only in $CO : H_2S$ mixtures, but also in the more realistic $H_2O : CO : H_2S$ interstellar ice analogs, to an equal or possibly greater extent.

4.4. *Comparing* OCS *Formation in Different Ices*

Figure 6 illustrates the differences in OCS production as a function of dose, sulfur donor species, and majority component of the ice. (In all cases, the sulfur donor was the limiting reactant for OCS formation.) Considering the water-free ices first, it is clear that CO provides a better source of the carbon-oxygen moiety in the product than does CO_2, regardless of the sulfur-containing parent. This is not surprising since the formation of OCS from CO_2 necessarily entails the fragmentation of both the CO_2 and the sulfur donor, followed by reaction of the appropriate fragments. Such a mechanism would be expected to decrease the probability of OCS product formation, compared to a similar process in CO, as observed and described above.

In CO-dominated ices, the OCS production efficiency follows the pattern of $H_2S > SO_2$ as sulfur donors. This corresponds to the relative ease of fragmentation expected from average bond energy values: H—S, 347 kJ mol^{-1} and O = S, 498 kJ mol^{-1} (Klotz & Rosenberg 1972, p. 60). This pattern is reinforced by the data indicated in Figure 8. The rates of destruction of the pure ices are also in the pattern $H_2S > SO_2$. In CO_2-dominated ices the pattern of OCS formation efficiency also appears consistent, with $H_2S > SO_2$. While this result is based on a peak-fitting procedure as described in § 3.3, the qualitative relationship seems quite reliable.

The introduction of H_2O as the majority species in the ice produced significant changes to the relative OCS formation efficiency by irradiation. Although the relative efficiency as a function of sulfur donor in H_2O-CO-sulfur samples followed the same pattern as in water-free CO ices, OCS production from H_2S was enhanced, while that from SO_2 was measurably depressed. In $H_2O : CO : H_2S$, the OCS/(original S) ratio was 0.12, whereas in the absence of H_2O the OCS/(original S) ratio was 0.08 for $CO : H_2S$ ices. Increased fragmentation of H_2S may occur because the more polar environment of the water matrix, compared to that of CO, may stabilize the fragmentation products. At the same time, the network of bonds in the H_2O-ice may limit the motion of the larger SO_2 degradation products; the mobile, light H atoms are not similarly hindered.

4.5. *Radiation Destruction of* OCS *and Precursors in* H_2O*-Free and* H_2O*-Rich Ices*

Figure 6 indicates that the amount of OCS in the ice varied as a function of dose; in most cases, the concentration rose to a peak and then fell off. As indicated by the spectra in Figure 7, the reason for the decrease in OCS concentration at higher doses was that OCS itself was destroyed by the radiation that also served to produce it. The fact that OCS could be completely fragmented by the radiation is apparent from the products identified in Figure 7—CS_2, SO_2, and the intermediate OCS_2, which itself grows and decays within the dosage range indicated. A comparison of the relative rates of destruction of the sulfur compounds on exposure to radiation is provided in Figure 8. To better illustrate the effect of H_2O on the process, the figure is divided into sections for pure ices and water-dominated ices. As mentioned above, the rate of destruction of pure ices of SO_2 and H_2S increased in that order, just as observed for these molecules serving as minor components in CO-dominated ices. Figure 8 indicates that OCS is even more prone to radiation-induced destruction than H_2S. Given the relative strengths of the O = C and H—S bonds, this is surprising, but may simply result from the stability of the degradation products SO_2 and CS_2, which are far less susceptible to the radiation. In addition, H_2S_2 may form during irradiation and act as an intermediate in the reformation of H_2S (Moore et al. 2007).

When trapped in water, the rates of destruction of SO_2 and H_2S change compared to the pure ice, both becoming much more vulnerable to the effect of the radiation. Unlike the pure materials, OCS, H_2S, and SO_2 in water behave quite similarly when irradiated.

4.6. *Astrophysical Implications*

The molecules we used to generate OCS in these experiments are CO and CO_2 mixed with H_2S and SO_2. Since all of these are known or suspected (in the case of H_2S) interstellar molecules, it is reasonable to expect that interstellar ices produce OCS when exposed to UV photons, cosmic rays, or other sources of high-energy radiation. We also have shown that H_2O-ice does not block OCS formation in three-component ices, such as $H_2O : CO : H_2S$ (See, for example, Table 3 and Fig. 4).

Our work shows that S-atom addition to CO is the likely path for OCS formation in binary, apolar CO- and CO_2-rich ices, as well as polar ices dominated by H_2O. In CO-rich icy interstellar mantles, S atoms could combine with CO to form OCS. In a CO_2-rich mantle, CO has to come from CO_2 dissociation, and so compared to CO-rich ices, we expect a lower OCS abundance for the same radiation exposure at 10 K, as observed in our experiments.

Interstellar ices rich in CO_2 are expected to produce CO_3 by processing with UV photons or other radiation sources. In such cases, our work shows that a strong OCS band around 2040–2050 cm^{-1} overlaps with a CO_3 absorbance in the same region. The CO_3 feature is more symmetrical, varies less in position (2044–2045 cm^{-1}), and has a smaller width (4.5–8.7 cm^{-1}) than the OCS absorbance (see Table 2), but unraveling these

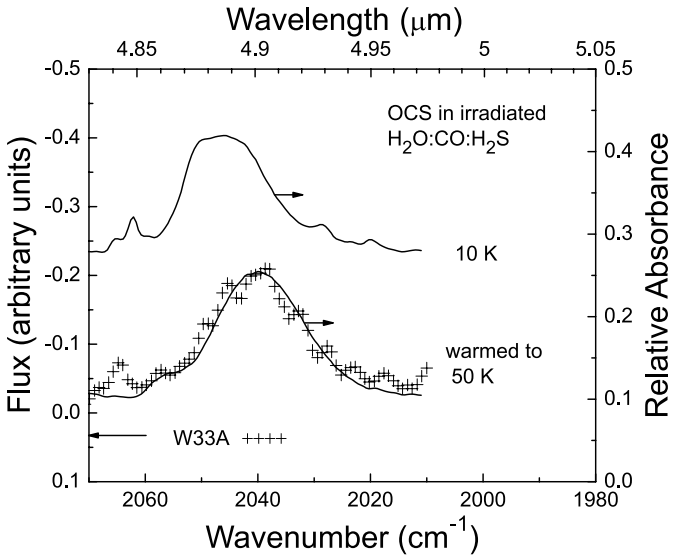

FIG. 10.—Comparison of the 4.9 μm feature of W33A with the OCS band of a $H_2O:CO:H_2S$ mixture irradiated at 10 K to $\sim$4 eV molecule^{-1}. The upper trace is from the ice after irradiation at 10 K while the lower one is the spectrum (*solid line*) of the same ice but after warming to 50 K.

two IR bands is difficult. This problem is not evident in CO-bearing laboratory ices since less CO_3 is formed in them.

The OCS band profile depends on the composition of the ice mixture in which the molecule is embedded. Palumbo et al. (1995, 1997) discussed OCS band shifts in unirradiated ices containing H_2O and CH_3OH. They concluded that OCS in an ice mantle with little or no water and rich in methanol best fit the W33A spectrum near 4.9 μm. In the present study we have documented, for the first time, the band position and shape of OCS formed in irradiated ices. We have shown that not only is the profile sensitive to initial ice composition, but that reference spectra of OCS in different unirradiated mixtures do not reproduce OCS positions, line shapes, or line widths in irradiated ices (Fig. 4).

Figure 10 compares the OCS band formed from irradiated $H_2O:CO:H_2S$ ice with the 4.90 μm feature of W33A observed with the *Infrared Space Observatory* (Gibb et al. 2000). At 10 K the OCS band at 2045 cm^{-1} is shifted to a larger wavenumber than seen for W33A. However, after warming the irradiated ice to 50 K the OCS band shifts to a lower wavenumber, and a good match to the observations is obtained. The W33A band in Figure 10 is at 2041 cm^{-1} and has a width $\sim$17.5 cm^{-1} (calculated using standard curve-fitting techniques), while the OCS absorbance for our 50 K ice is at 2039 cm^{-1} with a width of 18 cm^{-1}. Our laboratory ice ratio of $H_2O:CO$ is about 3 times that observed in W33A for the CO polar component (Gibb et al. 2000). Our laboratory radiation doses simulate about 10^7 yr of processing in a dense-cloud environment, and our 50 K ice temperature is consistent with the idea that W33A displays evidence of both thermal and energetic processing.

On the surfaces of icy satellites like Europa, where both CO_2 and SO_2 are known to exist in a relatively high radiation environment, OCS is a promising organosulfur molecule for future searches. Not only is OCS an astronomical target, it also is of astrobiological interest, since it has been demonstrated to promote prebiotic formation of peptides (Leman et al. 2004). Although the extension of the latter room-temperature work to Europa's temperatures (86–130 K) has not yet been studied, OCS appears to be an interesting molecule for prebiotic chemistry.

5. CONCLUSIONS

We have performed extensive experiments on OCS formation in proton-irradiated water-free and water-dominated ices containing CO and CO_2 as carbon sources and H_2S or SO_2 as sulfur sources. OCS is readily formed in each case. The formation efficiency is greater with CO-rich ices than CO_2-rich ices, and more OCS forms in both cases when H_2S is the source of S instead of SO_2. The formation of OCS in H_2O-dominated $H_2O:CO:H_2S$ ices might have been expected to be smaller than in $CO:H_2S$ samples, due simply to dilution by H_2O molecules. Our finding was of *greater* OCS formation in the presence of water-ice. More work is required to further examine this result. As indicated earlier, the mechanism of OCS formation appears to be the reaction of CO with free S atoms produced by fragmentation of the sulfur parent species. The radiation-induced destruction of H_2S, SO_2, and OCS also has been examined. Results indicate that while OCS is readily formed by irradiation, it is also easily destroyed on continued exposure to the high-energy source. In H_2O-dominated ices the radiolytic half-life of H_2S, SO_2, and OCS is $\sim$2 eV molecule^{-1}, corresponding to $\sim$7 million years in a cold dense interstellar cloud environment processed by cosmic-ray proton.

The spectral profile of the strong ν_3 band of OCS is highly dependent on ice composition and temperature. Furthermore, the OCS profile differs in irradiated ices from that observed in untreated ones. Thus, laboratory studies of unirradiated OCS ice mixtures alone may not provide adequate information for modeling and spectral fits. However, the spectra of radiation-processed ices can be used to our advantage in modeling efforts, as illustrated by our match of the 2040 cm^{-1} W33A feature with a laboratory spectrum of irradiated $H_2O:CO:H_2S$ at 50 K.

The identification of OCS in CO_2-dominated ices provides a further challenge, in that CO_3 formation from irradiation of the host ice is very facile, and a strong band of that molecule is frequently blended with the OCS signal. While the two features often cannot be resolved, the separate contributions of OCS and CO_3 can be unraveled by curve fitting based on the constant position and narrow width of the CO_3 band to distinguish it from the much broader and more variable signal due to OCS. It is the width in the 2040 cm^{-1} band that will help determine if the feature observed in CO_2-rich ices is due to OCS or to CO_3.

The authors acknowledge support through The Goddard Center for Astrobiology, and NASA's Planetary Atmospheres, Outer Planets, and Planetary Geology and Geophysics programs. In addition, we thank Steve Brown, Claude Smith, and Eugene Gerashchenko, members of the Radiation Laboratory at NASA Goddard, for operation of the accelerator. R. L. H. acknowledges support from NASA Grant NNG 05-GJ46G. M. M. S. gratefully acknowledges the Office of Naval Research for partial support of this work on funding document N0001407WR20077.

REFERENCES

Aydin, M., De Bruyn, W. J., & Saltzman, E. S. 2002, Geophy. Res. Lett., 29, 73
Bahou, M., & Lee, Y. P. 2001, J. Chem. Phys., 115, 10694
Bennett, C. J., Jamieson, C., Mebel, A. M., & Kaiser, R. I. 2004, Phys. Chem. Chem. Phys., 6, 735
Boogert, A. C. A., Schutte, W. A., Helmich, F. P., Tielens, A. G. G. M., & Wooden, D. H. 1997, A&A, 317, 929
Brucato, J. R., Palumbo, M. E., & Strazzulla, G. 1997, Icarus, 125, 135
Charnley, S. B. 1997, ApJ, 481, 396
Charnley, S. B., Ehrenfreund, P., & Kuan, Y.-J. 2001, Spectrochim. Acta, 57, 685

Charnley, S. B., Ehrenfreund, P., Millar, T. J., Boogert, A. C. A., Markwick, A. J., Butner, H. M., Ruiterkamp, R., & Rodgers, S. D. 2004, MNRAS, 347, 157
Geballe, T. R. 1991, MNRAS, 251, P24
Geballe, T. R., Baas, R., Greenberg, J. M., & Schutte, W. 1985, A&A, 146, L6
Gerakines, P. A., & Moore, M. H. 2001, Icarus, 154, 372
Gerakines, P. A., Schutte, W. A., & Ehrenfreund, P. 1996, A&A, 312, 289
Gibb, E. L., et al. 2000, ApJ, 536, 347
Grim, R. J. M., & Greenberg, J. M. 1987, ApJ, 321, L91
Hatchell, J., Thompson, M. A., Millar, T. J., & Macdonald, G. H. 1998, A&A, 338, 713
Hawkins, M., Almond, M. J., & Downs, A. J. 1985, J. Phys. Chem., 89, 3326
Hawkins, M., & Downs, A. J. 1984, J. Phys. Chem., 88, 1527
Hudgins, D. M., Sandford, S. A., Allamandola, L. J., & Tielens, A. G. G. M. 1993, ApJS, 86, 713
Hudson, R. L., & Moore, M. H. 1999, Icarus, 140, 451
———. 2000, A&A, 357, 787
———. 2004, Icarus, 172, 466
Hudson, R. L., Palumbo, M. E., Strazzulla, G., Moore, M. H., Cooper, J., & Sturmer, S. J. 2007, The Solar System Beyond Neptune (Tucson: Univ. Arizona Press)
Isoniemi, E., Pettersson, M., Khriachtchev, L., Lundell, J., & Räsänen, M. 1999, J. Phys. Chem. A, 103, 696
Jacox, M. E., & Milligan, D. E. 1971, J. Chem. Phys., 54, 919
Kamp, L. W., & Taylor, F. W. 1990, Icarus, 86, 510
Klotz, I. M., & Rosenberg, R. M. 1972, Chemical Thermodynamics (Menlo Park: Benjamin)
Leman, L., Orgel, L., & Ghadiri, M. R. 2004, Science, 306, 283
Lo, W. J., Chen, H.-F., Chou, P.-H., & Lee, Y.-P. 2004, J. Chem. Phys., 121, 12371
Lovas, F. J., & Dragoset, R. A. 2004, J. Phys. Chem. Ref. Data, 33, 177
Martin, S. 2005, The Evolution of Starbursts, ed. S. Hüttemeister et al. (Melville: AIP), 148
Moore, M. H. 1984, Icarus, 59, 114
Moore, M. H., & Hudson, R. L. 2003, Icarus, 161, 486
———. 2006, in IAU Symp. 231, Astrochemistry: Recent Successes and Current Challenges, ed. D. C. Lis, G. A. Blake, & E. Herbst (Cambridge: Cambridge Univ. Press), 247
Moore, M. H., Hudson, R. L., & Carlson, R. W. 2007, Icarus, 189, 409
Moore, M. H., Ferrante, R. F., & Nuth, J. A., III. 1996, Planet. Space Sci., 44, 927
Mumma, M. J., DiSanti, M. A., Dello Russo, N., Magee-Sauer, K., Gibb, E., & Novak, R. 2003, Adv. Space Res., 31, 2563
Okabe, H. 1978, Photochemistry of Small Molecules (New York: Wiley)
Palumbo, M. E., Geballe, T. R., & Tielens, A. G. G. M. 1997, ApJ, 479, 839
Palumbo, M. E., & Strazzulla, G. 1993, A&A, 269, 568
Palumbo, M. E., Tielens, A. G. G. M., & Tokunaga, A. T. 1995, ApJ, 449, 674
Salama, F., Allamandola, L. J., Witteborn, F. C., Cruikshank, D. P., Sandford, S. A., & Bregman, J. D. 1990, Icarus, 83, 66
Schriver-Mazzuoli, L. Schriver, A., & Chaabouni, H. 2003, Can. J. Phys., 81, 301
Smith, R. G. 1991, MNRAS, 249, 172
Trottier, A., & Brooks, R. L. 2004, ApJ, 612, 1214
Weaver, H. A. 1997, in IAU Symp. 178, Molecules in Astrophysics: Probes and Processes, ed. D. J. Jansen, M. R. Hogerheijde, & E. F. van Dishoeck (Cambridge: Cambridge Univ. Press), 205
Woodney, L. M., McMullin, J., & A'Hearn, M. F. 1997, Planet. Space Sci., 45, 717
Ziegler, J. F., Biersack, J. P., & Littmark, U. 1985, The Stopping and Range of Ions in Solids (Pergammon, New York) (see also http://www.srim.org)